Journal of Molecular Cell Biology (2024), 16(10), mjae047 https://doi.org/10.1093/jmcb/mjae047
Published online October 14, 2024

Article

Cohesin ring gates are specialized for meiotic cell division

Yuanyuan Liu[1], Bohan Liu[1], Ruirui Zhang[1], Zixuan Zhu[2], Li Zhao[1], Ruijie Jiang[1], Yinghao Wang[1], Feifei Qi[1], Ruoxi Wang[1], Huijie Zhao[1], Jun Zhou[1,2], and Jinmin Gao[1,2,*]

[1] Center for Cell Structure and Function, College of Life Sciences, Key Laboratory of Animal Resistance Biology of Shandong Province, Shandong Normal University, Jinan 250014, China
[2] Department of Genetics and Cell Biology, State Key Laboratory of Medicinal Chemical Biology, Haihe Laboratory of Cell Ecosystem, College of Life Sciences, Nankai University, Tianjin 300071, China
* Correspondence to: Jinmin Gao, E-mail: jinmingao@sdnu.edu.cn

Edited by Xuebiao Yao

Cohesin is a ring complex closed with structural maintenance of chromosome 1 (SMC-1), SMC-3, and a kleisin subunit, mediating sister chromatid cohesion in mitosis and meiosis. Kleisin N- and C-terminal domains interact with SMC-3 and SMC-1, forming two distinct cohesin gates. Whether these gates are specialized for mitosis and meiosis remains elusive. Here, we create *Caenorhabditis elegans* mutants that express chimeric proteins swapping N- and C-terminal domains between different kleisins to investigate how these gates are specialized for different cell division programs. Replacing the meiotic REC-8 N-terminus with that of a cell division-unrelated kleisin COH-1 or the mitotic kleisin sister chromatid cohesion protein 1 (SCC-1) disrupts inter-sister chromatid cohesion and causes severe meiotic defects. Swapping the REC-8 C-terminus with that of COH-1 or SCC-1 largely retains the meiotic functions of REC-8 but causes age-related chromosome abnormalities. A specialized C-terminus is also required for the functions of SCC-1. Furthermore, point mutations in the REC-8 C-terminus cause severe meiotic defects without impairing the SMC-1–kleisin interaction, suggesting an integrated SMC-1–kleisin gate. These findings suggest the requirements for specialized cohesin gates in different biological processes.

Keywords: *Caenorhabditis elegans*, cohesin, kleisin, meiosis, mitosis, REC-8

Introduction

Cohesin is an evolutionarily conserved ring complex that can topologically entrap DNA strands to exert a broad range of nuclear functions, including DNA replication, DNA damage repair, gene expression, and mitotic and meiotic chromosomal segregation. During mitosis, inter-sister chromatid cohesion ensures that duplicate chromosomes align properly at the metaphase plate, with separase-mediated cleavage resulting in their segregation. Two-step cohesion removal is required during meiosis, e.g. cohesin removal from chromosome arms during meiosis I and centromeric cohesin removal during meiosis II, allowing sequential chromosome segregation. Unlike mitosis, human meiosis has a prolonged prophase that can last decades from the initial cohesin establishment until the final two rounds of cohesin removal. There is increasing evidence that chromosome cohesin is lost as mammals age, which may underlie age-related aneuploidy in oocytes (Chiang et al., 2010; Lister et al., 2010; Duncan et al., 2012; Sakakibara et al., 2015; Zielinska et al., 2015, 2019; Liu and Gao, 2023). However, what cohesin features aid long-term maintenance remains unclear.

Core cohesin ring components include two structural maintenance of chromosome (SMC) proteins, SMC-1 and SMC-3, an α-kleisin subunit, and the kleisin-binding protein SA/sister chromatid cohesion protein 3 (SCC-3) (Ishiguro, 2019). SMC proteins contain two globular domains at each end, flanking a hinge domain with two rod-like coiled-coil arms. The hinge domain allows the folding of the molecule and interactions between its N- and C-terminal lobes, thereby forming a globular head domain. SMC-1 and SMC-3 interact through their hinge domains to form a V-shaped heterodimer. Their head domains further interact to form composite ABC-type ATPase domains. An α-kleisin subunit bridges the SMC ATPase lobes, with its N-terminus interacting

Received March 14, 2024. Revised October 3, 2024. Accepted October 13, 2024.

with the coiled-coil connection of the SMC-3 neck and its C-terminus interacting with the SMC-1 C-lobe, forming two distinct cohesin gates, i.e. kleisin N-gate and kleisin C-gate. SMC ATPase activity is critical for cohesin ring formation, and point mutations in Smc1 Walker A or B motifs that abolish adenosine triphosphate (ATP) binding dramatically reduce Scc1's ability to bind stably to Smc1/3 heterodimers *in vivo* (Arumugam et al., 2003; Weitzer et al., 2003). Recent studies have shown that the topological association and dissociation of the cohesin complex to DNA require SMC-3–kleisin gate opening and SMC ATPase activity (Higashi et al., 2020). SA/SCC-3 proteins stably bind to the kleisin subunits in the central region, mediating DNA binding and recruitment of cohesin regulators (Shintomi and Hirano, 2009; Liu et al., 2013; Murayama and Uhlmann, 2014; Li et al., 2018).

Most eukaryotes have evolutionarily conserved meiosis-specific cohesin subunits that are critical for successful meiosis by supporting synaptonemal complex (SC) assembly, crossover formation, and prolonged sister chromatid cohesion (Rankin, 2015; Ishiguro, 2019). While yeast only has one meiosis-specific cohesin subunit (Rec-8), metazoans tend to have multiple meiosis-specific kleisins; for example, the nematode *Caenorhabditis elegans* has three meiosis-specific kleisins REC-8, COH-3, and COH-4 (Severson and Meyer, 2014), and mammals have two meiosis-specific kleisins, REC-8 and RAD21L. Except for SMC-3, meiotic versions of the other core cohesin components are also present in some organisms, including SMC-1 and SA/SCC-3. Humans have meiosis-specific SMC-1B and STAG3, which are functional homologs of mitotic SMC-1A and STAG1/2, respectively. Although meiosis-specific cohesin components share conserved amino acid sequences with their mitotic homologs, they are not substitutable. Replacing Rec-8 with Scc1 in yeast during meiosis results in meiotic chromosomal segregation errors (Toth et al., 2000; Hsieh et al., 2020), and expressing Rec-8 during mitosis delays cellular proliferation (Buonomo et al., 2000). Moreover, *Smc1b* deletion in mice causes meiotic errors and infertility (Revenkova et al., 2004), and replacing *Smc1b* with *Smc1a* only partially rescues some phenotypes and meiosis still fails (Biswas et al., 2018). These observations suggest that different versions of cohesin subunits exist in mitosis and meiosis not only through the regulation of gene expression but also because they exert different functions. While their minor sequence differences may mediate these varied properties, the molecular basis for their distinct functions is still unclear.

Here, we investigated how cohesin gates are specialized for different cell division programs in *C. elegans* and found that both kleisin N-gate and kleisin C-gate are specialized for meiotic cell division. A specialized SMC-1–kleisin gate is required for prolonged cohesion maintenance during meiosis and the prevention of age-related chromosomal abnormalities. Furthermore, structural predictions and the creation of point mutations at the REC-8 C-terminus suggest that the SMC-1–kleisin gate not only serves as a connector but may have a mechanistic role impacting SMC head structure.

Results

Kleisin N- and C-terminal domains exhibit distinct evolutionary rates

Kleisins are highly conserved in their secondary structures, enabling the definition of their N- and C-terminal domain territories. To understand how meiotic cohesins are specialized for their functions, sequences of the kleisin subunits from four widely studied organisms, e.g. *Schizosaccharomyces pombe*, *C. elegans*, *Drosophila melanogaster*, and *Homo sapiens*, were aligned according to their three functional territories: the N-terminal domain that interacts with SMC-3, the central region that contains separase cleavage sites and binding sites for cohesin loading regulators, and the C-terminal domain that connects with the SMC-1 head domain (Figure 1A). These three territories do not show similar conservation patterns across species. Specifically, the N-termini of mitotic kleisins are highly conserved across the species, while their meiotic counterparts lose such conservation. The central region generally loses conservation both in mitotic and meiotic kleisins, suggesting this is a region highly evolved to adapt to various requirements for biological processes. Lastly, kleisin C-termini do not show a similar conservation pattern as the N-termini but are averagely more conserved between meiotic and mitotic subunits.

N-terminus-replaced REC-8 fails to establish sister chromatid cohesion

The nematode *C. elegans* has five kleisins, and three of them, REC-8, COH-3, and COH-4, are meiosis-specific, while sister chromatid cohesion protein 1 (SCC-1) is essential for mitosis. Another kleisin, COH-1, is ubiquitously expressed and is not required for both mitosis and meiosis (Supplementary Figure S1A; Pasierbek et al., 2001; Mito et al., 2003). In the *C. elegans* germline, REC-8, SCC-1, and COH-1 exhibited distinct expression patterns (Supplementary Figure S1B). Specifically, REC-8 was highly expressed before meiotic entry and remained consistently associated with chromosomes throughout the meiotic prophase. SCC-1 was hardly detected during the early meiotic prophase but was observed in the premeiotic tip (PMT) region and during the late meiotic prophase. In contrast to REC-8 and SCC-1, COH-1 was only detected during the late meiotic prophase and was absent in the PMT and the early meiotic prophase. To investigate whether the terminal domains of REC-8 were specialized for meiosis, the terminal domains of COH-1 and SCC-1 were substituted for those of REC-8 in this study.

Structural and complex prediction using AlphaFold showed that the N-terminal domains of REC-8, COH-1, and SCC-1 formed a similar binding pattern with SMC-3 neck helixes, with a more extended helix predicted for REC-8. To determine whether a specialized N-terminus is required for REC-8, we performed genome editing in *C. elegans* to replace the coding sequence of the N-terminal 95 amino acids (aa) of REC-8 with the N-terminal 89 aa of COH-1 or the N-terminal 86 aa of SCC-1. Structural prediction suggested this replacement retained the extended helix and docking similarly to SMC-3 neck helixes as the REC-8

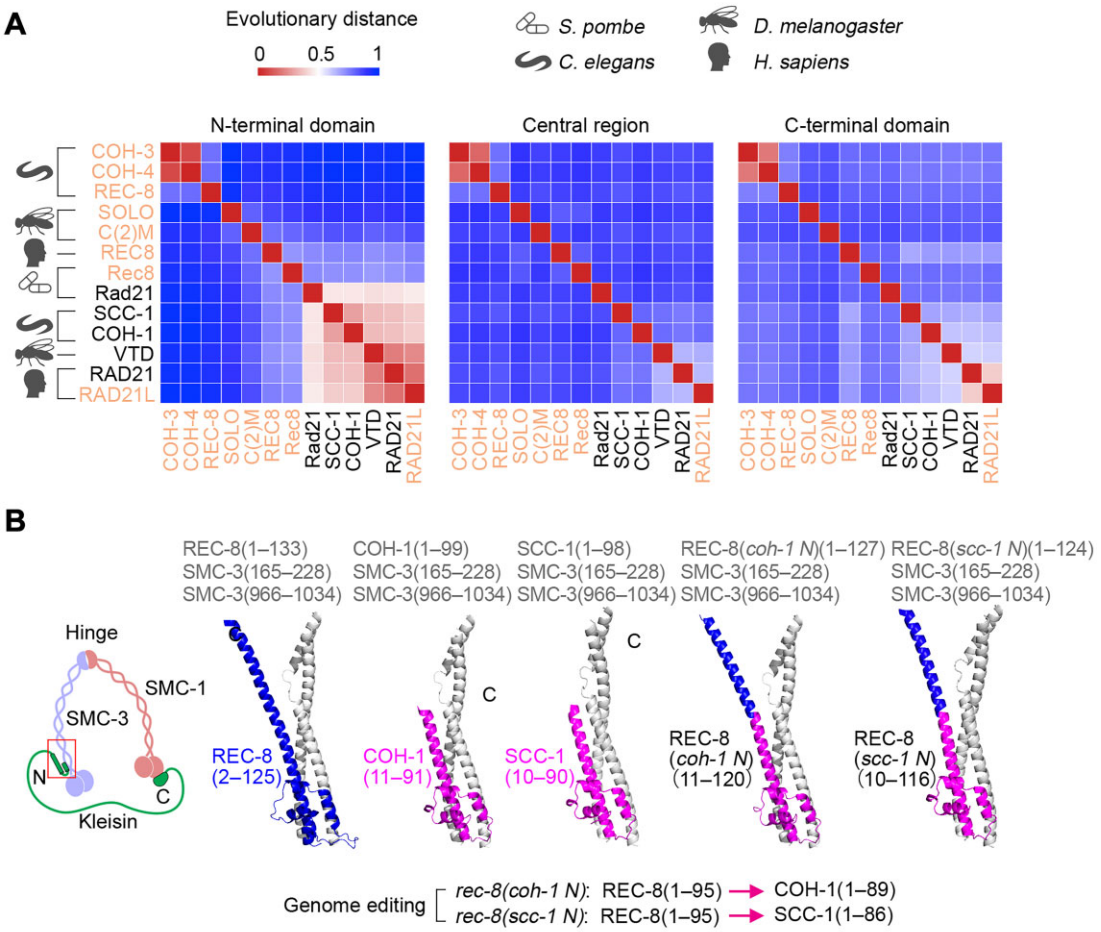

C

Genotype	Adult brood sizes (# of P0)	% Viable progeny (# of embryos)	% Males (# of adults)
wt	312 (14)	100 (4319)	0.05 (4367)
rec-8(coh-1 N)	5 (8)	7.0 (568)	20.0 (40)
rec-8(coh-1 N)/nT1	101 (6)	75.8 (799)	0.3 (606)
rec-8(scc-1 N)	15 (10)	11.1 (1345)	17.4 (149)
rec-8(scc-1 N)/nT1	200 (10)	70.9 (2803)	0.1 (2003)

Figure 1 Kleisin N- and C-terminal domains exhibit different evolutionary rates. (**A**) Evolutionary distances of different kleisin domains across the indicated organisms. Meiosis-specific kleisins are in orange. Alignments were performed using Clustal Omega with the neighbor-joining clustering method. (**B**) Prediction of complex formation between *C. elegans* kleisin N-termini and SMC-3 neck coiled coils by AlphaFold2. Sequence information used for the prediction is detailed at the top. Information on N-terminal domain swapping in *rec-8(coh-1 N)* and *rec-8(scc-1 N)* mutants is shown at the bottom. (**C**) Plate phenotypes of wildtype and N-terminus-replaced *rec-8* mutants.

or COH-1 N-terminus (Figure 1B). Interaction analysis in 293T cells confirmed that the SMC-3 head domain interacted with these kleisins, and replacing the N-terminal domain of REC-8 with that of COH-1 or SCC-1 did not impair its interaction with SMC-3 (Supplementary Figure S2).

Plate phenotype analyses of the generated *rec-8(coh-1 N)* and *rec-8(scc-1 N)* mutants suggest REC-8 functions were severely impaired (Figure 1C). While wildtype worms produced 100% viable progeny and >300 adult brood sizes, *rec-8(coh-1 N)* mutants had only 7% viable progeny and ~5 adult brood sizes, and *rec-8(scc-1 N)* mutants had 11% viable progeny with ~15 adult brood sizes. A high incidence of male offspring (Him) phenotype was also observed in both mutants, suggesting nondisjunction of X-chromosomes during meiosis. However, *rec-8(coh-1 N)/nT1* and *rec-8(scc-1 N)/nT1* heterozygotes showed high viable progeny (71%–76%) and no obvious Him phenotype, with lethality attributable to inviable *nT1* homozygotes. Thus, the N-terminal replacements had no obvious haploinsufficiency or dominant negative effects (Figure 1C).

Cytological analyses were further performed to reveal meiotic defects in *rec-8(coh-1 N)* mutants. Upon meiotic entry, chromosomes cluster together, forming a crescent-shaped organization in the transition zone nuclei in the germline (zone 1 of the meiotic prophase). This region corresponds to

the leptotene/zygotene stage. Chromosomes then redisperse throughout the nuclear periphery when cells progress to pachytene with complete synapsis (Figure 2A). Quantification of nuclei at different stages revealed a delay in progressing into pachytene in *rec-8(coh-1 N)* and *rec-8(scc-1 N)* mutants (Figure 2B; Supplementary Figure S3), suggesting synapsis defects. Immunostaining of SC lateral element/axis protein HTP-3 and central region component SYP-1 showed that most of the chromosome axes were associated with the SC central region (Figure 2C). Quantification of HTP-3 and SYP-1 tracks in *rec-8(coh-1 N)* mutants revealed mean numbers of ∼12 and ∼11, respectively, nearly double those observed in the wildtype. Similarly, *rec-8(scc-1 N)* mutants had mean track numbers of ∼11 for HTP-3 and ∼10 for SYP-1 (Figure 2D). These observations suggest that the SC central region was ubiquitously assembled on separated homologous chromosomes, i.e. between sister chromatids, consistent with the previous observation (Cahoon et al., 2019).

Moreover, examination of crossover designation marker COSA-1 showed nearly 12 foci per nucleus in both *rec-8(coh-1 N)* and *rec-8(scc-1 N)* mutants (Figure 2E and F), similar to SYP-1 track number, suggesting that each SC track may efficiently guide inter-sister crossover formation. At diakinesis, increased numbers of 4′,6-diamidino-2-phenylindole (DAPI)-stained bodies were observed (Figure 2G and H), suggesting a lack of inter-homologous crossovers and disruption of sister chromatid cohesion.

To examine the expression and localization of the mutated REC-8, we generated two REC-8 antibodies using the central region (aa 346–502) and the C-terminal 200-aa segment of REC-8 as antigens (Supplementary Figure S4A). The two antibodies worked for western blot and immunostaining, respectively. Western blot analysis of whole worm lysates with the first antibody confirmed the expression of all mutated REC-8 variants, although levels were reduced for REC-8(*coh-1 N*) and REC-8(*scc-1 N*) (Supplementary Figure S4B). Immunostaining with the second antibody further validated the expression of the mutated REC-8 (Supplementary Figure S4C). *rec-8(coh-1 N)* mutants showed an abundant REC-8 signal in nuclei before meiotic entry but was not detected on chromosomes during the meiotic prophase, suggesting that the N-terminus-replaced REC-8 failed to establish sister chromatids cohesion upon meiotic entry. Together, these findings suggest that the N-terminus of REC-8 is specialized for meiosis, and it cannot be substituted by the N-terminus of a cell division-unrelated kleisin.

C-terminus-substituted rec-8 mutants show mild defects during the meiotic prophase

To gain insights into whether the SMC-1–kleisin gate is also specialized for meiosis, we created *rec-8(coh-1 C)* and *rec-8(scc-1 C)* mutants via genome editing to replace the coding sequences of the REC-8 C-terminus with those of COH-1 or SCC-1. Complex prediction revealed that the C-termini of these kleisins adopted similar structures, docking at the same location on the SMC-1 head (Figure 3A). Deleting the last two β-sheets within the SMC-1 head domain, which were predicted to interact with kleisin C-termini, effectively abolished their interactions (Supplementary Figure S5A and B). Additionally, replacing the C-terminal domain of REC-8 with that of COH-1 or SCC-1 did not impair its interaction with the SMC-1 head (Supplementary Figure S5C and D). Compared to the N-terminus-replaced mutants, the *rec-8(coh-1 C)* and *rec-8(scc-1 C)* mutants showed milder plate phenotypes (Figure 3B). Specifically, *rec-8(coh-1 C)* mutants had 40% viable progeny and ∼80 adult brood sizes, accompanied by a Him phenotype (∼15% males), while *rec-8(scc-1 C)* mutants had 45% viable progeny and ∼120 adult brood sizes (Figure 3B), which were much higher than those observed in the N-terminus-replaced mutants. These phenotypes suggest that the C-terminus-replaced REC-8 is at least partially functional *in vivo*.

Cytological analyses revealed milder meiotic defects in *rec-8(coh-1 C)* and *rec-8(scc-1 C)* mutants compared to phenotypes observed in the N-terminus-replaced mutants. A slightly extended transition zone was observed in *rec-8(coh-1 C)* and *rec-8(scc-1 C)* mutants compared to the wildtype (Figure 3C; Supplementary Figure S3). Immunostaining of HTP-3 and SYP-1 showed the presence of unsynapsed chromosomes in the mid-pachytene nuclei of *rec-8(coh-1 C)* mutants (Figure 4A). However, most of the pachytene nuclei in the mutants still formed six SC tracks, similar to wildtype and *rec-8(scc-1 C)* mutants (Figure 4B). Consistently, six COSA-1 foci (Figure 4C) and six DAPI-stained bodies (Figure 4D) were observed for most nuclei at late pachytene and diakinesis, respectively, in these mutants, similar to that in wildtype worms, suggesting crossover and bivalent formation are largely normal in *rec-8(coh-1 C)* and *rec-8(scc-1 C)* mutants. Immunostaining of REC-8 in *rec-8(coh-1 C)* mutants revealed the association of mutated REC-8 with chromosomes during the meiotic prophase. However, potentially due to the disrupted antigen region in mutated REC-8, the signal was significantly reduced (Supplementary Figure S4C). These cytological analyses suggest that C-terminus-replaced REC-8 largely supports meiotic functions during the early meiotic prophase, although it may have defects in cohesin maintenance and/or removal during later stages that may cause the reduced viability and Him phenotype.

C-terminus-substituted rec-8 mutants show age-related meiotic chromosome abnormalities

To further assess how the altered SMC-1–kleisin gate affects the long-term maintenance of cohesion, we examined meiotic progression in germlines of aged worms (5 days post-L4). Interestingly, although synapsis defects and crossover designation remained unchanged with age in *rec-8(coh-1 C)* mutants (Supplementary Figure S6), defects in bivalent formation and structure maintenance were observed in the oocytes of the aged mutants (Figure 4E). While six DAPI-stained bodies were consistently observed in aged wildtype worms, the number of DAPI-stained bodies in the oocytes of aged *rec-8(coh-1 C)*

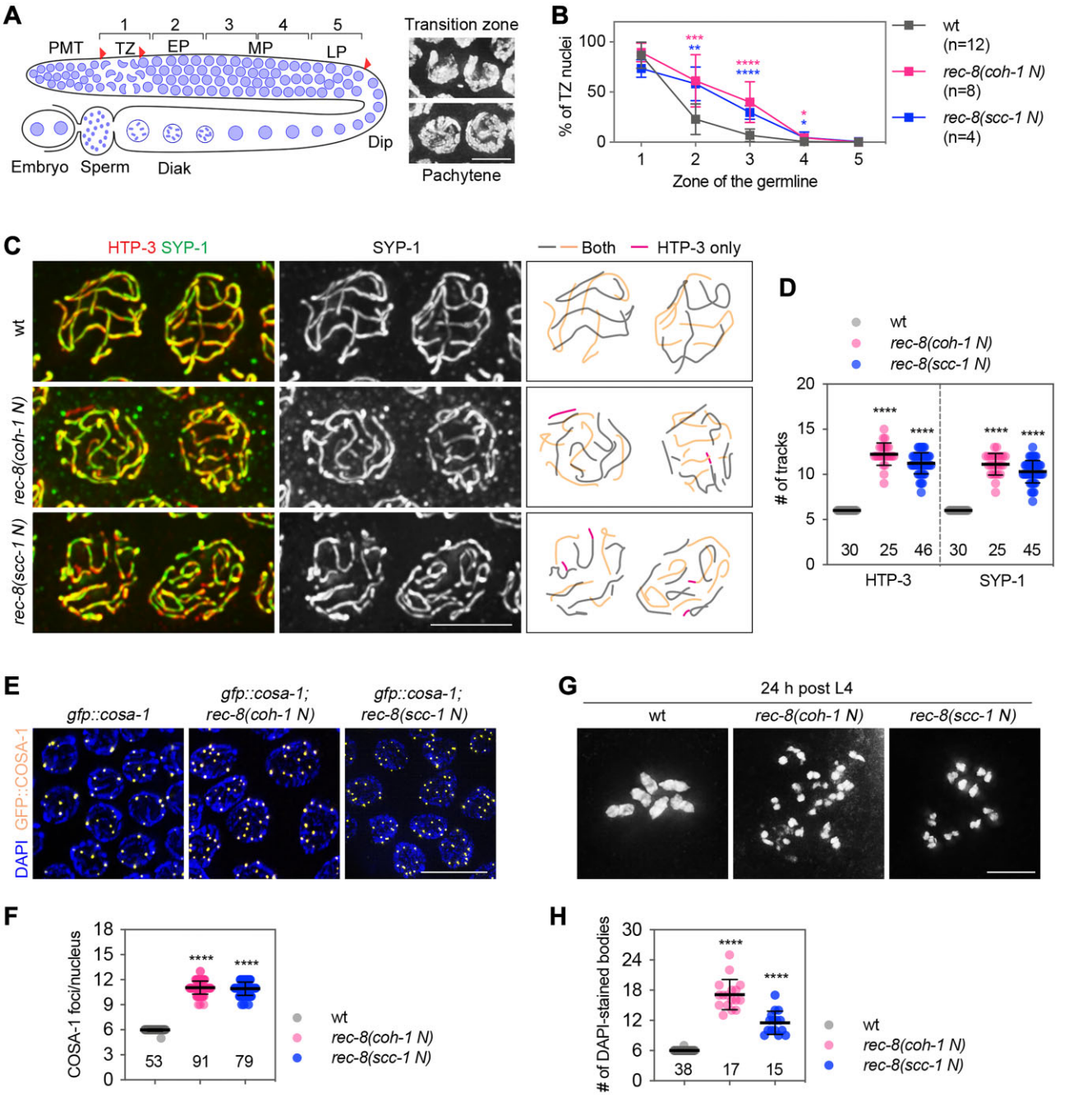

Figure 2 A specialized N-terminus is required for the meiotic functions of REC-8. (**A**) Schematic of meiotic prophase substages in the *C. elegans* germline and the position of the equally divided five zones. TZ, transition zone. The right panels show representative TZ and pachytene nuclei. Scale bar, 5 μm. (**B**) Quantification of TZ nuclei across gonad zones. Data points are mean ± SD. *$P < 0.05$, **$P < 0.01$, ***$P < 0.001$, ****$P < 10^{-4}$, two-tailed unpaired *t*-test. (**C**) Co-immunostaining of HTP-3 (red) and SYP-1 (green) in zone 4 pachytene nuclei. HTP-3/SYP-1 tracks are illustrated on the right, with tracks containing both shown in gray or orange and HTP-3-only tracks shown in red. Scale bar, 5 μm. (**D**) Quantification of HTP-3 and SYP-1 tracks in zone 4 nuclei. Lines are mean ± SD. ****$P < 10^{-8}$, two-tailed unpaired *t*-test. (**E**) GFP::COSA-1 (yellow) focus formation in late pachytene nuclei. Scale bar, 10 μm. (**F**) Quantification of GFP::COSA-1 in late pachytene nuclei. Lines are mean ± SD. ****$P < 10^{-8}$, two-tailed unpaired *t*-test. (**G**) DAPI-stained bodies in diakinesis nuclei. Scale bar, 5 μm. (**H**) Quantification of DAPI-stained bodies in −1 oocytes. Lines are mean ± SD. ****$P < 10^{-8}$, two-tailed unpaired *t*-test.

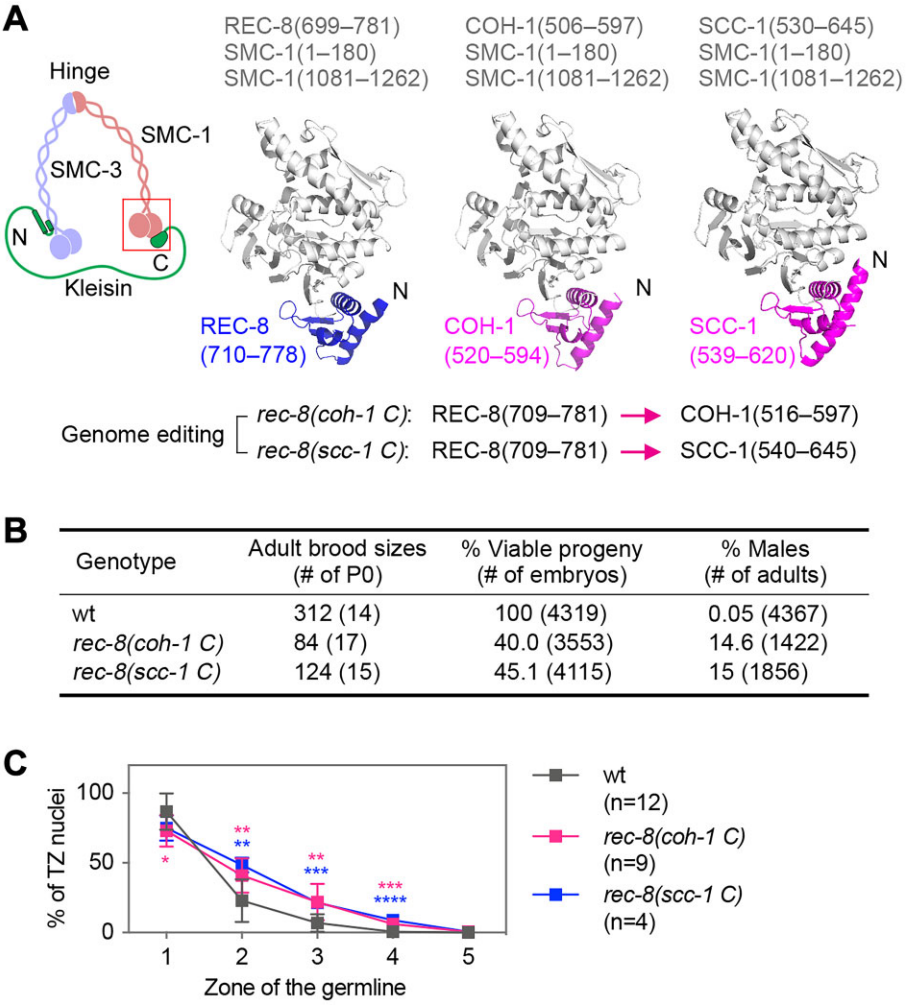

Genotype	Adult brood sizes (# of P0)	% Viable progeny (# of embryos)	% Males (# of adults)
wt	312 (14)	100 (4319)	0.05 (4367)
rec-8(coh-1 C)	84 (17)	40.0 (3553)	14.6 (1422)
rec-8(scc-1 C)	124 (15)	45.1 (4115)	15 (1856)

Figure 3 Predicted SMC-1–kleisin interactions and generation of C-terminus-replaced *rec-8* mutants. (**A**) Prediction of complex formation between the SMC-1 head domain and the REC-8 or COH-1 C-terminal domain. Sequence information used for prediction is shown at the top and information on the C-terminal domain swapping in *rec-8(coh-1 C)* and *rec-8(scc-1 C)* mutants is detailed at the bottom. (**B**) Plate phenotypes of wildtype, *rec-8(coh-1 C)*, and *rec-8(scc-1 C)* mutants. (**C**) Quantification of TZ nuclei in gonads of the indicated genotypes. Data points are mean ± SD. $*P < 0.05$, $**P < 0.01$, $***P < 0.001$, $****P < 10^{-4}$, two-tailed unpaired *t*-test.

mutants increased (Figure 4E). In aged *rec-8(scc-1 C)* mutants, an increase in the number of DAPI-stained bodies in oocytes was not apparent. However, abnormal bivalent structures were observed in both *rec-8(coh-1 C)* and *rec-8(scc-1 C)* aged mutants, with apparent gaps separating the bivalent into multiple lobes (Figure 4E and F), suggesting a potential weakening of cohesion. These phenotypes suggest that the REC-8-specific C-terminus is critical for the prevention of age-related nondisjunction.

A mitosis-specific C-terminus is essential for the functions of SCC-1

We also sought to examine whether a specialized C-terminus is required for the proper functions of the mitotic kleisin SCC-1, which is ubiquitously expressed and crucial for various biological processes, including gene expression, DNA damage repair, and cell division. Its expression pattern overlaps with COH-1 in some tissues in the worms. To aid in exploring the specificity of the SCC-1 C-terminus, we created an *scc-1(coh-3 C)* mutant (Figure 5A), in which the SCC-1 C-terminus coding sequence was replaced with that of COH-3, which is functionally redundant with COH-4 and is expressed only during the early meiotic prophase in the germline, showing minimal overlap in the expression pattern with SCC-1 (Severson and Meyer, 2014). Thus, such replacement would likely maximize the defects in the domain-swapping mutants if a specialized C-terminus is necessary. Homozygous *scc-1(coh-3 C)* mutants, isolated from the progeny of heterozygote hermaphrodites, developed into adults with protruded vulvas (data not shown) and failed to lay eggs (Figure 5B). However, heterozygotes carrying *scc-1(coh-3 C)* allele and mIn1 balancer showed plate phenotypes similar to the wildtype (Figure 5B).

Cytological analysis showed that the gonads were small and contained very few diplotene or diakinesis nuclei in the

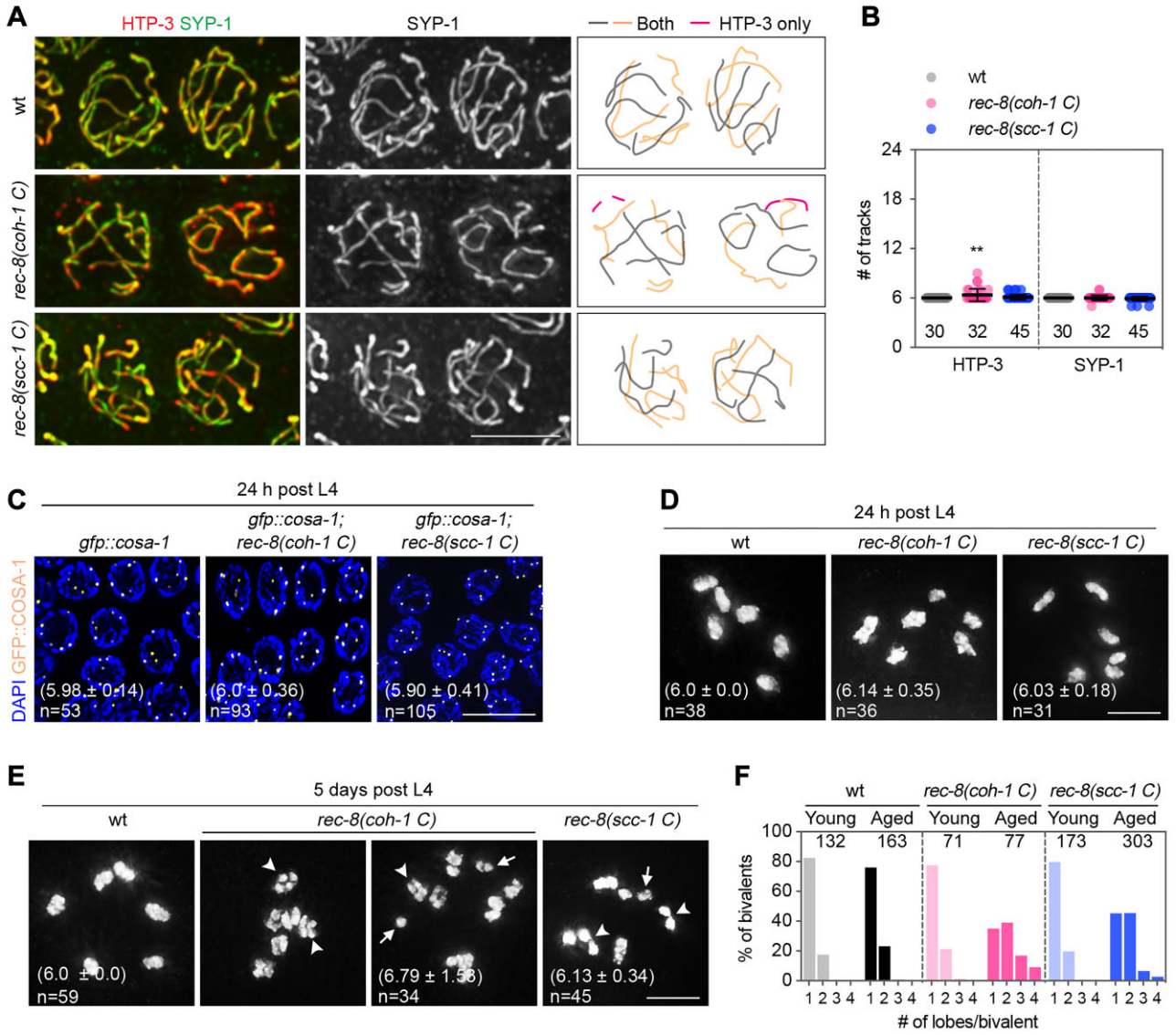

Figure 4 C-terminus-replaced REC-8 supports meiotic progression with milder defects. (**A**) Co-immunostaining of HTP-3 (red) and SYP-1 (green) in zone 4 nuclei of the indicated genotypes. HTP-3/SYP-1 tracks are illustrated on the right. Scale bar, 5 μm. (**B**) Quantification of HTP-3 and SYP-1 tracks in zone 4 nuclei. Lines are mean ± SD. $^{**}P = 0.0082$, two-tailed unpaired *t*-test. (**C**) GFP::COSA-1 (yellow) focus formation in late pachytene nuclei. Mean ± SD of COSA-1 foci per nucleus and nuclei scored are indicated. Scale bar, 10 μm. (**D**) Diakinesis DAPI-stained bodies in the young adults. Mean ± SD of DAPI-stained bodies per oocyte and oocytes scored are indicated. Scale bar, 5 μm. (**E**) Diakinesis DAPI-stained bodies in aged adults. Arrowheads indicate impaired cohesion in bivalents exhibiting multi-lobes. Arrows indicate univalent or separated sister chromatids. Mean ± SD of DAPI-stained bodies per oocyte and oocytes scored are indicated. Scale bar, 5 μm. (**F**) Distribution of bivalents exhibiting 1–4 distinguishable lobes in late diakinesis oocytes. Only oocytes containing six DAPI-stained bodies were scored, and the numbers of the bivalents analyzed are indicated.

mutants (Figure 5C and D). Occasionally, bright DAPI-stained clouds, likely representing degrading nuclei, were observed in the proximal gonad arm region in the mutants, suggesting that the mitotic kleisin also plays essential roles in germ cell development. Interestingly, although germ cell development was severely disrupted in *scc-1(coh-3 C)* mutants, complete synapsis was still achieved in the pachytene nuclei (Figure 5E), suggesting that the mitotic cohesin might not be required for the formation of core meiotic structures. While a functional antibody is unavailable to directly assess the expression of the chimeric SCC-1, expression and interaction analyses of C-terminal-replaced REC-8 suggest that the chimeric SCC-1 is likely still properly expressed and capable of forming cohesin rings. However, these cohesin rings appear to be misregulated and unable to support the essential functions of mitotic cohesin.

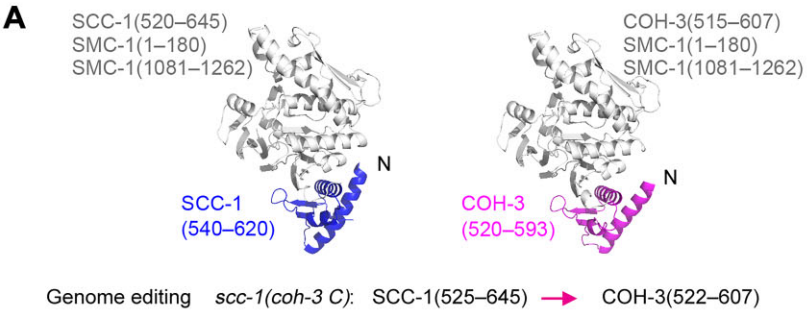

B

Genotype	Adult brood sizes (# of P0)	% Viable progeny (# of embryos)	% Males (# of adults)
wt	312 (14)	100 (4319)	0.05 (4367)
scc-1(coh-3 C)	0 (10)	0 (0)	0 (0)
scc-1(coh-3 C)/mIn1	261 (10)	99.3 (2581)	0 (2563)

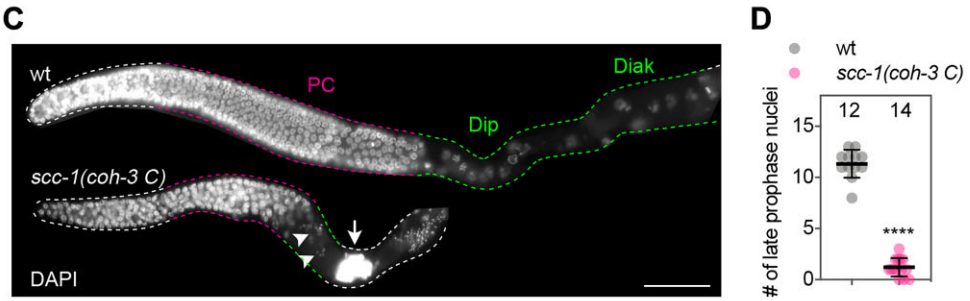

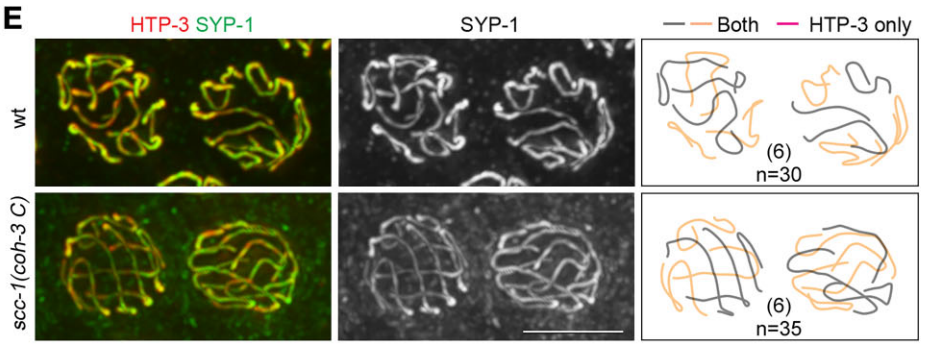

Figure 5 A specialized C-terminal domain is required for the functions of mitotic SCC-1. (**A**) Prediction of complex formation between the SMC-1 head domain and SCC-1 or COH-3 C-termini. Sequence information used for prediction is shown at the top and information on C-terminal domain swapping in the *scc-1(coh-3 C)* mutant is shown at the bottom. (**B**) Plate phenotypes of wildtype and *scc-1(coh-3 C)* mutants. (**C**) DAPI staining of gonads from the indicated genotypes. Arrowheads indicate late prophase nuclei, and the arrow indicates the DAPI cloud of a potentially degrading nucleus. Scale bar, 50 μm. (**D**) Quantification of nuclei numbers at diplotene and diakinesis. Lines represent mean ± SD. ****$P < 10^{-8}$, two-tailed unpaired *t*-test. (**E**) Co-immunostaining of HTP-3 (red) and SYP-1 (green) in pachytene nuclei of the indicated genotypes. Six HTP-3/SYP-1 tracks are consistently observed per nucleus. Scale bar, 5 μm.

C. elegans kleisin C-termini may differentially impact SMC-1 head structure

It has been shown that yeast cohesin ATPase activity can be stimulated by the Scc-1 C-terminus (Arumugam et al., 2006). Such stimulation may depend on specific conformational changes within the ATPase head domain induced by the kleisin C-terminus. Indeed, by aligning the predicted structures of the SMC-1 head domain with and without kleisin engagements, we found that the engagements of kleisin C-termini caused conformational changes within the head domain, with the extent of these changes varying among different kleisins (Figure 6). Specifically, mitotic SCC-1 and meiotic REC-8 C-termini caused ~1.8 Å shift of the neck helixes when a set of β-sheets on the other side of the head domain was used as the aligning

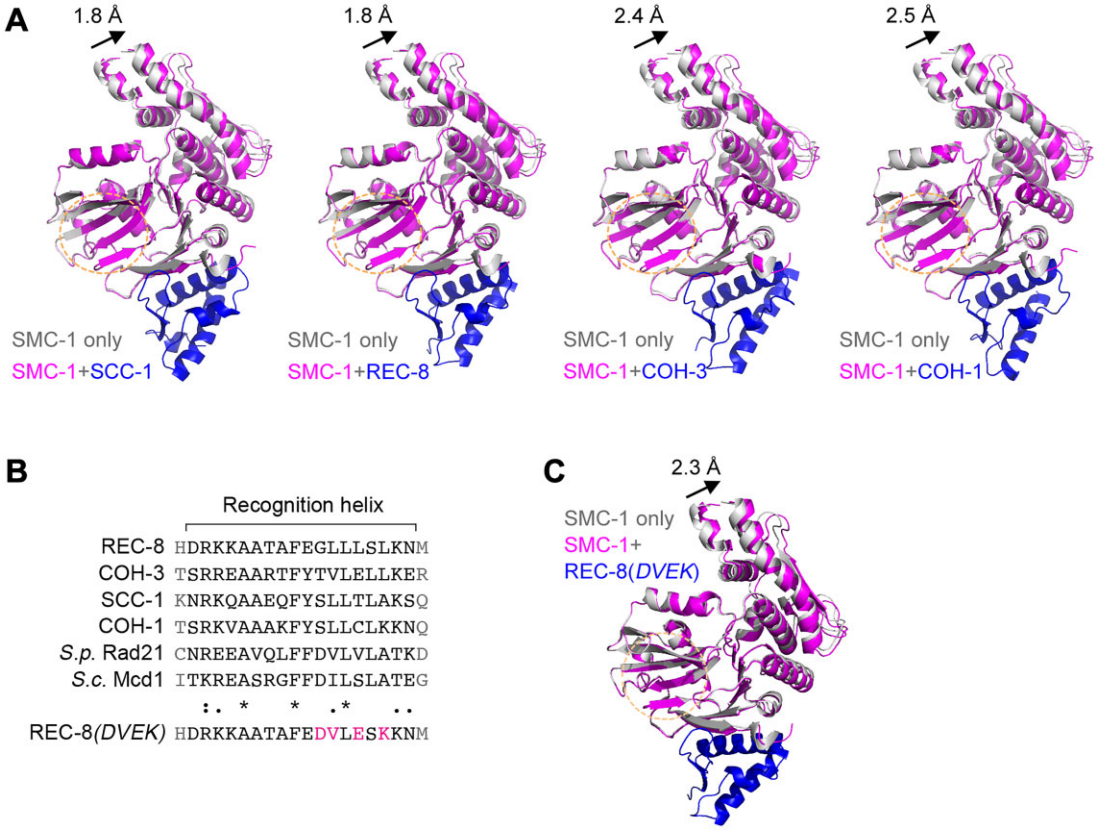

Figure 6 Potential conformational alterations of the SMC-1 head domain induced by kleisin C-termini. (**A**) SMC-1 head domain structure predictions were performed as in Figure 3A, with or without kleisin sequences. The structure of the SMC-1 head domain alone (gray) was aligned to structures with the engagements of kleisin C-termini (magenta and blue). Yellow-circled β-sheets were used as the reference for alignment. Black arrows indicate the shifts of the coiled coils at the neck region. (**B**) Sequence alignment of the recognition helix from *C. elegans* and yeast kleisins. Point mutations introduced in REC-8(*DVEK*) are highlighted in red. *S.p.*, *S. pombe*; *S.c.*, *Saccharomyces cerevisiae*. (**C**) Structural alignment of the SMC-1 head domain with (magenta) or without (gray) engagement of the REC-8(*DVEK*) C-terminus (blue).

reference. In comparison, the engagements of COH-3 and COH-1 C-termini caused a greater shift, 2.4–2.5 Å, of the neck helixes with the same alignment setting. Interestingly, the degree of conformational alterations correlated with the severity of the phenotypes observed in *rec-8(coh-1 C)* and *rec-8(scc-1 C)* mutants. Specifically, brood size reduction, defects in synapsis, and bivalent formation were more pronounced in the *rec-8(coh-1 C)* mutants compared to the *rec-8(scc-1 C)* mutants (Figures 3B and 4A, B, D, and E). This suggests that conformational changes induced by kleisin C-termini may partially explain their distinct functions. However, additional mechanisms are likely involved, as similar conformational changes were induced by REC-8 and SCC-1, yet defects were still present in the *rec-8(scc-1 C)* mutants. Potential mechanisms could include differences in post-translational modifications, differential binding partners, or distinct regulators within the C-terminal domain.

We further examined whether engagements of different kleisin C-termini may cause conformational changes to the human SMC head. Engagements of the three kleisin C-termini with the mitotic SMC-1A all caused significant shifts of the neck helixes when a set of β-sheets on the other side of the head domain were used as the aligning reference (Supplementary Figure S7A). Approximately 3.6 Å shift was observed when RAD21 was engaged, and engagements of meiotic RAD21L and REC-8 caused greater shifts, 6.7 Å and 6.2 Å shifts, respectively. However, engagements of kleisin C-termini with the meiotic SMC-1B caused only minor shifts compared to that with SMC-1A, ranging from 0.3 Å to 0.9 Å (Supplementary Figure S7B). These predictions suggest the mitotic and meiotic SMC-1 head domains may be differentially impacted by the engagements of kleisins, suggesting a potential common mechanism by which kleisin C-gates are specialized for various biological processes.

Point mutations in the REC-8 C-terminus cause cohesin dysfunction without impairing the SMC-1–kleisin interaction

Within the kleisin C-terminus, a conserved 'recognition helix' was suggested to mediate the major contacts with SMC-1 through hydrophobic interactions (Haering et al., 2004; Gligoris et al., 2014). We further tested how the hydrophobicity of the recognition helix might contribute to the SMC-1–kleisin interaction and cohesin functions. Based on amino acid homology in the paralogs or homologs, we designed a

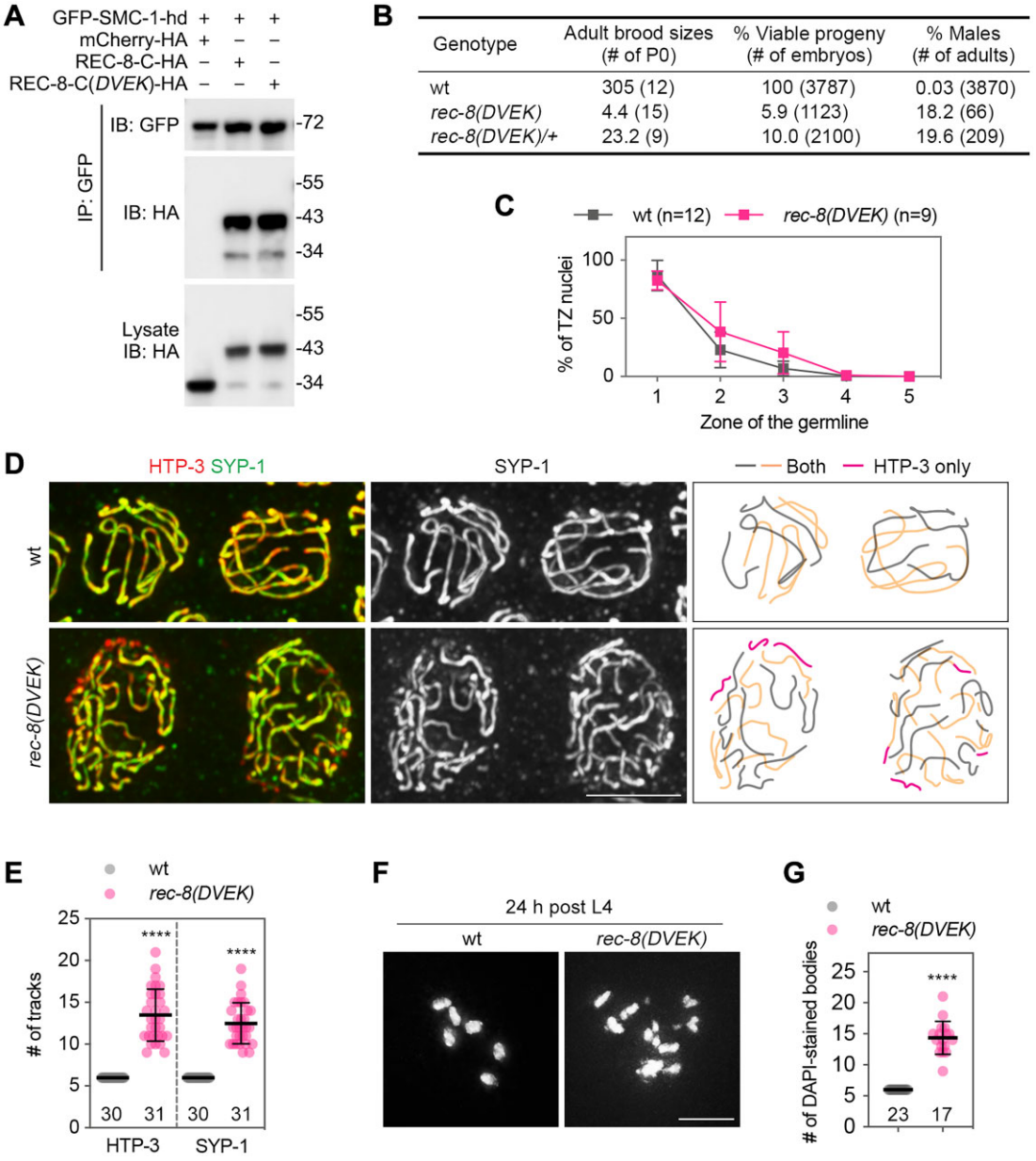

Genotype	Adult brood sizes (# of P0)	% Viable progeny (# of embryos)	% Males (# of adults)
wt	305 (12)	100 (3787)	0.03 (3870)
rec-8(DVEK)	4.4 (15)	5.9 (1123)	18.2 (66)
rec-8(DVEK)/+	23.2 (9)	10.0 (2100)	19.6 (209)

Figure 7 *DVEK* mutations in REC-8 C-termini cause severe cohesin dysfunction. (**A**) Interactions between the SMC-1 head domain and wildtype or mutated REC-8 C-termini. Tagged proteins were co-expressed in 293T cells, and their interactions were examined by immunoprecipitation and western blotting. (**B**) Plate phenotypes of wildtype and *rec-8(DVEK)* mutants. (**C**) Quantification of TZ nuclei in gonads of the indicated genotypes. Data points are mean ± SD. (**D**) Co-immunostaining of HTP-3 (red) and SYP-1 (green) in zone 4 nuclei of the indicated genotypes. HTP-3/SYP-1 tracks are illustrated on the right. Scale bar, 5 μm. (**E**) Quantification of HTP-3 and SYP-1 tracks in zone 4 nuclei. Lines are mean ± SD. ****$P < 10^{-8}$, two-tailed unpaired *t*-test. (**F**) Diakinesis DAPI-stained bodies in young adults of the indicated genotypes. Scale bar, 5 μm. (**G**) Quantification of DAPI-stained bodies in −1 oocytes. Lines are mean ± SD. ****$P < 10^{-8}$, two-tailed unpaired *t*-test.

REC-8(*DVEK*) mutant, in which four less conserved amino acids were mutated to reduce the hydrophobicity at the recognition helix (Figure 6B). Structure prediction and alignment suggest the engagement of the mutated REC-8 C-terminus was predicted to cause ∼2.3 Å shift of the neck helixes of SMC-1, which was slightly greater than that induced by wildtype REC-8 C-terminus (1.8 Å) (Figure 6C).

To experimentally test the impacts of altered hydrophobicity of the recognition helix on SMC-1 interaction and *in vivo* functions of REC-8, the same *DVEK* mutations were introduced into a REC-8 mammalian expression construct and a *rec-8(DVEK) C. elegans* mutant. Biochemical analysis showed that such mutations did not impair the interaction with the SMC-1 head domain (Figure 7A), consistent with the fact that the mutations

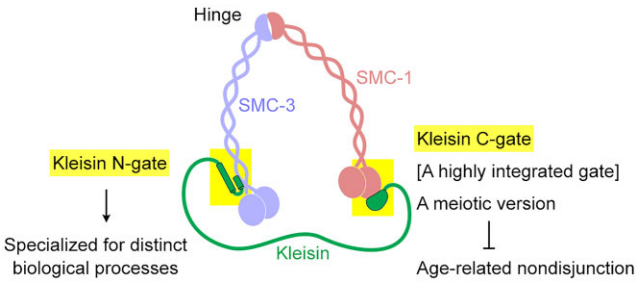

Figure 8 Specialization of cohesin gates for distinct biological processes. Within the cohesin ring, SMC-3–kleisin and SMC-1–kleisin gates are specialized for distinct biological processes. The kleisin C-gate is highly integrated, and a meiotic version of the kleisin C-gate is required for normal meiosis and the prevention of age-related nondisjunction.

did not disrupt the essential amino acids predicted to mediate contacts with the SMC-1 head. However, plate phenotype analysis of *rec-8(DVEK)* homozygous mutants revealed extremely reduced viability (5.9% vs. 100% in the wildtype) and a strong Him phenotype (18.2% males) (Figure 7B), suggesting disrupted *in vivo* functions in sister chromatid cohesion, homologous synapsis, and other related processes. Cytological analysis revealed a slight delay of the germ cells to progress into pachytene (Figure 7C), and co-immunostaining of HTP-3 and SYP-1 showed that most of the chromosome axes were decorated with the SC central region (Figure 7D). However, quantification of the SC showed significantly increased track numbers of HTP-3 and SYP-1 (Figure 7E), suggesting SC formation between sister chromatids. At diakinesis, the number of DAPI-stained bodies also increased (Figure 7F and G), suggesting defective bivalent formation in the *rec-8(DVEK)* mutants. These observations suggest that the mutated REC-8 causes severe cohesin dysfunction *in vivo*. Consistently, REC-8 failed to associate with the meiotic chromosomes during the meiotic prophase, although its diffused signal was observed before meiotic entry (Supplementary Figure S4C).

It is worth noting that the phenotypes observed for *rec-8(DVEK)* are not identical to those of *rec-8(coh-1 N)* or *rec-8(scc-1 N)* mutants. Of note, *rec-8(DVEK)* heterozygote mutants showed severe plate phenotypes with only 10% viability and ~20% males, suggesting a dominant negative impact of the *DVEK* mutation, which was not observed for the N-terminus-replaced *rec-8* mutant alleles. Moreover, analysis of RAD-51 kinetics in the germline also revealed more severe defects in DNA double-strand break repair in *rec-8(DVEK)* mutants compared to other *rec-8* mutants (Supplementary Figure S8). These differences suggest the different natures of cohesin dysfunction among these mutants. In conclusion, our data suggest that the SMC-1–kleisin interaction not only serves as a connector between the kleisin and the cohesin head but may also impact SMC head conformation and is specialized for various regulations (Figure 8).

Discussion

While the mitotic program is highly conserved between species, the meiotic program shows more diversity with varied time lengths of the meiotic prophase, and different sets of meiosis-specific cohesin subunits are required in different organisms, which may explain the highly evolved meiotic kleisins compared to their mitotic counterparts. Metazoans possess multiple meiosis-specific kleisin subunits, and only one seems critical for prolonged cohesion maintenance, namely REC-8 cohesin. However, the other meiotic cohesins also play essential roles during the meiotic prophase, including axis formation, SC assembly, and meiotic recombination. Evidence from multiple organisms suggests that meiotic cohesion can only be established during the premeiotic S-phase (Tachibana-Konwalski et al., 2010; Burkhardt et al., 2016; Gyuricza et al., 2016; Woglar et al., 2020). It must be maintained for varied periods during the meiotic prophase in different organisms. The non-turnover property of REC-8 cohesin presents a challenge for the prolonged maintenance of inter-sister chromatid cohesion and provides the basis for theories of age-related nondisjunction in females (Webster and Schuh, 2017).

Specialized kleisin domains resistant to specific regulations may be essential for prolonged meiotic cohesin maintenance. During mitotic cell division, cohesin is removed from the majority of chromosome arms via a cleavage-independent pathway during late G2 or pro-metaphase, the so-called 'prophase pathway' (Haarhuis et al., 2014). Several kinases and the cohesin-releasing factor WAPL are required during this process (Nishiyama et al., 2010, 2013). Similarly, cohesin is removed via a prophase-like pathway during meiosis in various organisms (De et al., 2014; Brieno-Enriquez et al., 2016; Challa et al., 2016; Crawley et al., 2016). Our unpublished data reveal that dissociation of green fluorescent protein (GFP)-tagged SMC-1 (SMC-1::GFP) from the meiotic chromosomes occurs after pachytene exit in *C. elegans*, suggesting the removal of a subset of cohesin complexes. However, diffusion of REC-8::GFP during the late meiotic prophase was not observed, suggesting that REC-8 cohesin may be resistant to some regulations during the late prophase, benefiting the prolonged maintenance of meiotic cohesin.

The middle regions of kleisins are largely unstructured and mediate the recruitment of multiple cohesin regulators for loading and unloading (Shintomi and Hirano, 2009; Liu et al., 2013; Murayama and Uhlmann, 2014; Li et al., 2018). It is also the region that contains separase cleavage sites that mediate cohesin removal upon anaphase initiation. Thus, it makes sense to speculate that the kleisin middle region plays a fundamental role in determining the specialized functions of kleisins in various biological processes. However, our current analyses revealed that both the N-termini and C-termini of kleisins also critically impact their specialized functions.

Recent studies have started to reveal the molecular mechanisms of topological loading and unloading of cohesin complexes, which depend on the engagement and disengagement of cohesin head domains that are coupled with

ATP hydrolysis cycles (Elbatsh et al., 2016; Çamdere et al., 2018; Wang et al., 2018; Higashi et al., 2020; Shi et al., 2020). Structural analysis has revealed how ATP hydrolase cycles are linked to SMC-3–kleisin gate opening through a mechanistic regulation (Muir et al., 2020). The N-termini may play a direct role in regulating cohesion establishment, with structural variations of the N-termini potentially enabling the proper loading of cohesin during specific processes. In *rec-8(coh-1 N)* and *rec-8(scc-1 N)* mutants, the normal loading of REC-8 cohesin at meiotic entry is disrupted, causing the separation of sister chromatids and failures in bivalent formation and accurate meiotic chromosome segregation. This disruption explains the observed plate and cytological phenotypes.

A specialized meiotic kleisin C-terminus may provide the stability required for the prolonged meiosis program (Figure 8). The SMC-1–kleisin interaction has been revealed as a prerequisite for the SMC-3–kleisin N interaction (Haering et al., 2004), and the opening of the SMC-1–kleisin gate may completely dissociate the complex from the chromosomes. Therefore, a specialized kleisin C-terminus might be essential to prevent premature disassembly of the complex. Consistently, age-related chromosome abnormalities were observed in the C-terminus-replaced *rec-8* mutants. Engagements of different kleisin C-termini may result in varied SMC ATPase activity, and an increased hydrolase activity may be correlated to increased instability of the cohesin complex. Furthermore, structural variations of kleisin C-termini may provide specialized regulations in different biological processes. Thus, stability and specialized regulation may together determine the maintenance of cohesin. In *rec-8(coh-1 C)* and *rec-8(scc-1 C)* mutants, homologous synapsis and crossover formation are largely normal. However, these mutants still exhibit relatively high Emb and Him phenotypes, indicating errors in meiotic chromosome segregation. These errors may partially be attributed to weakened cohesion during the late meiotic prophase, leading to abnormal bivalent structures and subsequent errors. Additionally, it remains unclear whether specific regulation of the SMC-1–kleisin gate exists during meiosis, beyond the established mechanisms of stepwise cohesin removal mediated by separase cleavage. A specialized C-terminus in REC-8 may therefore be crucial for establishing and maintaining proper chromosome structure throughout meiosis.

In mammals, multiple meiosis-specific subunits of the cohesin complex exist and might be coevolved, forming a specialized SMC-1–kleisin gate that promotes the stability of meiotic cohesin during the prolonged meiotic prophase. The engagements of subunits for different cell division programs might have altered ATPase activity, causing instability of the 'unmatched' subunits. Interestingly, age-related nondisjunction phenotype was also observed in the *Smc1b* knockout mouse model (Hodges et al., 2005), which could be related to an altered SMC ATPase activity. Given the highly integrated SMC-1–kleisin gate, gene variants that cause changes in critical amino acids involved in proper conformational changes and ATPase activation during SMC-1–kleisin engagements might cause cohesin dysfunction and maintenance defects. Identifying cohesin variants that cause meiotic defects and age-related nondisjunction is of translational significance for preventing reproductive diseases.

Materials and methods

C. elegans genetics and culture

N2 Bristol was used as the wildtype strain, and all mutants used in this study were derived from the N2 background. Worms were cultured at 20°C on nematode growth medium plates. The *rec-8* and *scc-1* mutant strains were created by CRISPR/Cas9 genome editing (detailed in Supplementary Materials and methods). A complete list of the worm strains used in this study can be found in Supplementary material. The *C. elegans* strains generated in this study are available from the corresponding author.

Plate phenotyping

To score egg viability and male progeny, L4 hermaphrodites were singled onto individual plates, and their eggs were counted immediately after each laying period (every 24 h). Surviving progeny and males were scored when worms reached the adult stage.

Protein structure prediction, visualization, and alignment

Protein multimer complex prediction was performed with ColabFold using AlphaFold2 and AlphaFold2-multimer (Mirdita et al., 2022). The top-ranked model for each structure or complex was selected for further comparisons or alignments. Structure visualization and alignment were performed with PyMOL, and only amino acids with a high confidence score (pLDDT $>$ 60) were visualized.

Immunofluorescence microscopy

Unless otherwise specified, all analyses were performed on 24 h post-L4 adults grown at 20°C. Gonad dissection, fixation, immunostaining, and DAPI counterstaining were performed as described previously (Zhang et al., 2020; Wang et al., 2024). The following primary antibodies were used: goat anti-SYP-1 (1:1000 dilution) (Clemons et al., 2013), guinea pig anti-HTP-3 (1:500 dilution) (Goodyer et al., 2008), mouse anti-REC-8 (1:200 dilution, customized antibody from GenScript), and rabbit anti-RAD-51 (1:10000 dilution, SDIX). All fluorescent dye-conjugated secondary antibodies were used at 1:200 dilution, including donkey anti-goat-Alexa488, donkey anti-guinea pig-Cy3, donkey anti-rabbit-Alexa488 (Jackson ImmunoResearch Laboratories), and goat anti-mouse-Alexa594 (Abcam). Fluorescence images were captured through whole nuclei at 200 nm intervals on a DeltaVision OMX microscope system with a 60$\times$ (NA 1.42) objective lens using SoftWoRx software (Applied Precision) in conventional imaging mode and deconvolved using a conservative algorithm with 10 iterations. Fluorescence microscope images shown were maximum-intensity projections through 3D data stacks of whole nuclei. Adobe Photoshop software was used to adjust the brightness and/or contrast of the images and to illustrate SC tracks in pachytene nuclei.

Detecting protein interactions via mammalian cell expression

Plasmid construction was performed using the homologous recombination method with ConExpress II One Step Cloning Kit (Vazyme, C112) and verified by DNA sequencing (detailed in Supplementary Materials and methods). Plasmids of the SMC-1 head and kleisin C-termini were pairwise co-transfected into 293T cells cultured in Dulbecco's modified Eagle's medium supplemented with 10% fetal calf serum at 37°C in a humidified atmosphere with 5% CO_2. Polyethyleneimine reagent (Sigma Aldrich) was used for plasmid transfection. Cells were lysed after 24 h in cell lysis buffer composed of 50 mM Tris–HCl (pH 7.4), 150 mM NaCl, 1 mM EDTA, 1 mM EGTA, 1% Nonidet P-40, 1 mM β-glycerophosphate, and a protease inhibitor mixture (Roche Diagnostics). Interactions between co-transfected proteins were examined by immunoprecipitation with anti-GFP nanoantibody agarose beads (Nuoyi Biology) and western blot analysis. The following primary and secondary antibodies were used: mouse anti-HA (1:2000 dilution, Sigma-Aldrich), chicken anti-GFP (1:2000 dilution, Abcam), horseradish peroxidase (HRP)-conjugated anti-mouse antibody (1:5000 dilution, Cell Signaling), and HRP-conjugated anti-chicken antibody (1:5000 dilution, Proteintech).

Supplementary material

Supplementary material is available at *Journal of Molecular Cell Biology* online.

Acknowledgements

We thank M. Colaiácovo (Harvard Medical School) and M. Zetka (McGill University) for the SYP-1 and HTP-3 antibodies.

Funding

This work was supported by grants from the National Natural Science Foundation of China (32022018 and 32370780) and the National Key Research and Development Program of China (2021YFA1101001). Some strains were provided by the Caenorhabditis Genetic Center (CGC), which is funded by National Institutes of Health (NIH) Office of Research Infrastructure Programs (P40 OD010440).

Conflict of interest: none declared.

Author contributions: methodology: Y.L. and J.G.; investigation: Y.L., B.L., R.Z., Z.Z., L.Z., R.J., Y.W., F.Q., R.W., and J.G.; writing: Y.L., J.G., and J.Z.; funding acquisition: J.G. and J.Z.; resources: J.G., J.Z., and H.Z.; and supervision: J.G.

References

Arumugam, P., Gruber, S., Tanaka, K., et al. (2003). ATP hydrolysis is required for cohesin's association with chromosomes. Curr. Biol. *13*, 1941–1953.

Arumugam, P., Nishino, T., Haering, C.H., et al. (2006). Cohesin's ATPase activity is stimulated by the C-terminal Winged-Helix domain of its kleisin subunit. Curr. Biol. *16*, 1998–2008.

Biswas, U., Stevense, M., and Jessberger, R. (2018). SMC1α substitutes for many meiotic functions of SMC1β but cannot protect telomeres from damage. Curr. Biol. *28*, 249–261.e4.

Brieno-Enriquez, M.A., Moak, S.L., Toledo, M., et al. (2016). Cohesin removal along the chromosome arms during the first meiotic division depends on a NEK1–PP1γ–WAPL axis in the mouse. Cell Rep. *17*, 977–986.

Buonomo, S.B., Clyne, R.K., Fuchs, J., et al. (2000). Disjunction of homologous chromosomes in meiosis I depends on proteolytic cleavage of the meiotic cohesin Rec8 by separin. Cell *103*, 387–398.

Burkhardt, S., Borsos, M., Szydlowska, A., et al. (2016). Chromosome cohesion established by Rec8–cohesin in fetal oocytes is maintained without detectable turnover in oocytes arrested for months in mice. Curr. Biol. *26*, 678–685.

Cahoon, C.K., Helm, J.M., and Libuda, D.E. (2019). Synaptonemal complex central region proteins promote localization of pro-crossover factors to recombination events during Caenorhabditis elegans meiosis. Genetics *213*, 395–409.

Çamdere, G., Carlborg, K.K., and Koshland, D. (2018). Intermediate step of cohesin's ATPase cycle allows cohesin to entrap DNA. Proc. Natl Acad. Sci. USA *115*, 9732–9737.

Challa, K., Lee, M.S., Shinohara, M., et al. (2016). Rad61/Wpl1 (Wapl), a cohesin regulator, controls chromosome compaction during meiosis. Nucleic Acids Res. *44*, 3190–3203.

Chiang, T., Duncan, F.E., Schindler, K., et al. (2010). Evidence that weakened centromere cohesion is a leading cause of age-related aneuploidy in oocytes. Curr. Biol. *20*, 1522–1528.

Clemons, A.M., Brockway, H.M., Yin, Y., et al. (2013). akirin is required for diakinesis bivalent structure and synaptonemal complex disassembly at meiotic prophase I. Mol. Biol. Cell *24*, 1053–1067.

Crawley, O., Barroso, C., Testori, S., et al. (2016). Cohesin-interacting protein WAPL-1 regulates meiotic chromosome structure and cohesion by antagonizing specific cohesin complexes. eLife *5*, e10851.

De, K., Sterle, L., Krueger, L., et al. (2014). Arabidopsis thaliana WAPL is essential for the prophase removal of cohesin during meiosis. PLoS Genet. *10*, e1004497.

Duncan, F.E., Hornick, J.E., Lampson, M.A., et al. (2012). Chromosome cohesion decreases in human eggs with advanced maternal age. Aging Cell *11*, 1121–1124.

Elbatsh, A.M.O., Haarhuis, J.H.I., Petela, N., et al. (2016). Cohesin releases DNA through asymmetric ATPase-driven ring opening. Mol. Cell *61*, 575–588.

Gligoris, T.G., Scheinost, J.C., Burmann, F., et al. (2014). Closing the cohesin ring: structure and function of its Smc3–kleisin interface. Science *346*, 963–967.

Goodyer, W., Kaitna, S., Couteau, F., et al. (2008). HTP-3 links DSB formation with homolog pairing and crossing over during C. elegans meiosis. Dev. Cell *14*, 263–274.

Gyuricza, M.R., Manheimer, K.B., Apte, V., et al. (2016). Dynamic and stable cohesins regulate synaptonemal complex assembly and chromosome segregation. Curr. Biol. *26*, 1688–1698.

Haarhuis, J.H., Elbatsh, A.M., and Rowland, B.D. (2014). Cohesin and its regulation: on the logic of X-shaped chromosomes. Dev. Cell *31*, 7–18.

Haering, C.H., Schoffnegger, D., Nishino, T., et al. (2004). Structure and stability of cohesin's Smc1–kleisin interaction. Mol. Cell *15*, 951–964.

Higashi, T.L., Eickhoff, P., Sousa, J.S., et al. (2020). A structure-based mechanism for DNA entry into the cohesin ring. Mol. Cell *79*, 917–933.e9.

Hodges, C.A., Revenkova, E., Jessberger, R., et al. (2005). SMC1β-deficient female mice provide evidence that cohesins are a missing link in age-related nondisjunction. Nat. Genet. *37*, 1351–1355.

Hsieh, Y.P., Makrantoni, V., Robertson, D., et al. (2020). Evolutionary repair: changes in multiple functional modules allow meiotic cohesin to support mitosis. PLoS Biol. *18*, e3000635.

Ishiguro, K.I. (2019). The cohesin complex in mammalian meiosis. Genes Cells *24*, 6–30.

Li, Y., Muir, K.W., Bowler, M.W., et al. (2018). Structural basis for Scc3-dependent cohesin recruitment to chromatin. eLife *7*, e38356.

Lister, L.M., Kouznetsova, A., Hyslop, L.A., et al. (2010). Age-related meiotic segregation errors in mammalian oocytes are preceded by depletion of cohesin and Sgo2. Curr. Biol. *20*, 1511–1521.

Liu, H., Rankin, S., and Yu, H. (2013). Phosphorylation-enabled binding of SGO1–PP2A to cohesin protects sororin and centromeric cohesion during mitosis. Nat. Cell Biol. *15*, 40–49.

Liu, Y., and Gao, J. (2023). Reproductive aging: biological pathways and potential interventive strategies. J. Genet. Genomics *50*, 141–150.

Mirdita, M., Schutze, K., Moriwaki, Y., et al. (2022). ColabFold: making protein folding accessible to all. Nat. Methods *19*, 679–682.

Mito, Y., Sugimoto, A., and Yamamoto, M. (2003). Distinct developmental function of two Caenorhabditis elegans homologs of the cohesin subunit Scc1/Rad21. Mol. Biol. Cell *14*, 2399–2409.

Muir, K.W., Li, Y., Weis, F., et al. (2020). The structure of the cohesin ATPase elucidates the mechanism of SMC–kleisin ring opening. Nat. Struct. Mol. Biol. *27*, 233–239.

Murayama, Y., and Uhlmann, F. (2014). Biochemical reconstitution of topological DNA binding by the cohesin ring. Nature *505*, 367–371.

Nishiyama, T., Ladurner, R., Schmitz, J., et al. (2010). Sororin mediates sister chromatid cohesion by antagonizing Wapl. Cell *143*, 737–749.

Nishiyama, T., Sykora, M.M., Huis in 't Veld, P.J., et al. (2013). Aurora B and Cdk1 mediate wapl activation and release of acetylated cohesin from chromosomes by phosphorylating sororin. Proc. Natl Acad. Sci. USA *110*, 13404–13409.

Pasierbek, P., Jantsch, M., Melcher, M., et al. (2001). A Caenorhabditis elegans cohesion protein with functions in meiotic chromosome pairing and disjunction. Genes Dev. *15*, 1349–1360.

Rankin, S. (2015). Complex elaboration: making sense of meiotic cohesin dynamics. FEBS J. *282*, 2426–2443.

Revenkova, E., Eijpe, M., Heyting, C., et al. (2004). Cohesin SMC1β is required for meiotic chromosome dynamics, sister chromatid cohesion and DNA recombination. Nat. Cell Biol. *6*, 555–562.

Sakakibara, Y., Hashimoto, S., Nakaoka, Y., et al. (2015). Bivalent separation into univalents precedes age-related meiosis I errors in oocytes. Nat. Commun. *6*, 7550.

Severson, A.F., and Meyer, B.J. (2014). Divergent kleisin subunits of cohesin specify mechanisms to tether and release meiotic chromosomes. eLife *3*, e03467.

Shi, Z., Gao, H., Bai, X.C., et al. (2020). Cryo-EM structure of the human cohesin–NIPBL–DNA complex. Science *368*, 1454–1459.

Shintomi, K., and Hirano, T. (2009). Releasing cohesin from chromosome arms in early mitosis: opposing actions of Wapl–Pds5 and Sgo1. Genes Dev. *23*, 2224–2236.

Tachibana-Konwalski, K., Godwin, J., van der Weyden, L., et al. (2010). Rec8-containing cohesin maintains bivalents without turnover during the growing phase of mouse oocytes. Genes Dev. *24*, 2505–2516.

Toth, A., Rabitsch, K.P., Galova, M., et al. (2000). Functional genomics identifies monopolin: a kinetochore protein required for segregation of homologs during meiosis I. Cell *103*, 1155–1168.

Wang, R., Li, J., Tian, Y., et al. (2024). The dynamic recruitment of LAB proteins senses meiotic chromosome axis differentiation in C. elegans. J. Cell Biol. *223*, e202212035.

Wang, X., Hughes, A.C., Brandão, H.B., et al. (2018). In vivo evidence for ATPase-dependent DNA translocation by the Bacillus subtilis SMC condensin complex. Mol. Cell *71*, 841–847.e5.

Webster, A., and Schuh, M. (2017). Mechanisms of aneuploidy in human eggs. Trends Cell Biol. *27*, 55–68.

Weitzer, S., Lehane, C., and Uhlmann, F. (2003). A model for ATP hydrolysis-dependent binding of cohesin to DNA. Curr. Biol. *13*, 1930–1940.

Woglar, A., Yamaya, K., Roelens, B., et al. (2020). Quantitative cytogenetics reveals molecular stoichiometry and longitudinal organization of meiotic chromosome axes and loops. PLoS Biol. *18*, e3000817.

Zhang, Z., Xie, S., Wang, R., et al. (2020). Multivalent weak interactions between assembly units drive synaptonemal complex formation. J. Cell Biol. *219*, e201910086.

Zielinska, A.P., Bellou, E., Sharma, N., et al. (2019). Meiotic kinetochores fragment into multiple lobes upon cohesin loss in aging eggs. Curr. Biol. *29*, 3749–3765.e7.

Zielinska, A.P., Holubcova, Z., Blayney, M., et al. (2015). Sister kinetochore splitting and precocious disintegration of bivalents could explain the maternal age effect. eLife *4*, e11389.

Received March 14, 2024. Revised October 3, 2024. Accepted October 13, 2024.